

Photoelectron holographic derivative transform for increased range of atomic images

S. H. Xu, H. S. Wu, M. Keeffe, Y. Yang, H. Cruguel, and G. J. Lapeyre
*Physics Department, Montana State University, Bozeman, Montana 59717**

(Received 8 August 2000; revised manuscript received 28 August 2001; published 25 January 2002)

A transform- k derivative spectra (KDS) transform—is introduced for construction of an atomic-structure image from photoelectron diffraction data. A phenomenological theory is used to show that the transform of spectrum derivatives enhances the image peaks by the square of the emitter-scatter distance when used in conjunction with the small cone method. In comparison with the standard transform used in photoelectron holography, the KDS transform allows more distant neighbors (scatterers) to be “seen” by the emitter and suppresses strong forward scattering. The ability to experimentally observe more neighbors of a photoelectron emitter expands the applicability of holographic imaging. The procedure is applied to experimental data obtained from the As/Si(111)-(1×1) and C₂H₄/Si(100)-(2×1) surface structures. The letter results show that C₂H₄ adsorption does not break the Si dimer bond.

DOI: 10.1103/PhysRevB.65.075410

PACS number(s): 61.14.Nm, 61.14.Qp

The determination of the positions of atoms at a surface has been one of the more difficult surface problems to solve. Photoelectron holographic imaging (PHI) using photoelectron diffraction (PHD) data has achieved notable successes in determining adsorbate structures and surface reconstruction structures.^{1–12} The technique is appealing, because it directly gives the position of atoms neighboring the electron emitter. The data are inverted to give an atomic image function whose peaks are frequently only very close to the emitter. As a result of the small number, the assignment of atoms to the peaks in the image may be difficult. We present a modification to the inversion which produces more peaks in the image at greater distances from the emitter. In this paper, several examples are presented.

The inversion uses angle-resolved photoemission data for the core level of interest. For each angle the intensity of the emission is measured as a function of wave number k (the photon energy). The angles used are uniformly distributed over the electron-emission hemisphere. Typically, 70–80 directions are measured with about 25 k points for each direction. Typical spectra are shown in Refs. 2 and 5. The data are first transformed with respect to the wave number, and the second transform is with respect to the angle.²

We introduce a transform where the derivative of the data is used in the transform. The wave-number k derivative-spectrum (KDS) transform successfully yields neighbors at greater distances from the emitter. The PHI images obtained by the KDS transform yield not only the first-nearest-neighbor and the second-nearest-neighbor (SNN) atomic images, but also the third-nearest-neighbor (TNN) images or even more greatly distant images. As a result, this method makes it easier to assign a unique atomic structure to the PHI image.

A short explanation of why the KDS transform works is given, and then two applications to experimental data are described where additional neighbors in the image are shown. The first application is for As on Si(111), where TNN images are found. The second is ethylene on Si(100) which was very recently published in Ref. 5. The Si atoms in the second layer (SNN image) are now seen. Now using bulk Si-Si distances for the second-layer image peaks, a determination of values for the C-C bond and Si-Si dimer lengths are

obtained. The value indicates that the Si dimer bond is not broken by chemisorption, an issue that has received some attention.

The essence of the analysis is to show that the image intensity obtained by transforming the derivative of the spectra is a factor of R^2 larger than the image intensity obtained by transforming the experimental spectra itself; \mathbf{R} is the image-space variable. This behavior is obtained only when the small-cone method is used in the angular transform. If the image obtained by the standard inversion is multiplied by R^2 —a different procedure—no image improvement is found.

According to photoelectron diffraction theory,^{2,10} we write a descriptive equation for the object wave, Ψ_O , and the reference wave, Ψ_R , in terms of an effective scattering factor $A(\mathbf{k}, \hat{r}_j)$ and the phase factor $kr_j(1 - \hat{k} \cdot \hat{r}_j)$, where k is the photoelectron wave number and \mathbf{r}_j is the position of the j th scatterer. The diffraction intensity $I(k, \hat{k})$ and its normalization for the interference effect $\chi(k, \hat{k})$ obey the relations

$$\begin{aligned} \chi(k, \hat{k}) &= |\Psi_O|^2 / |\Psi_R|^2 - 1 = I(k, \hat{k}) / |\Psi_R|^2 - 1 \\ &= \sum_j A(\mathbf{k}, \hat{r}_j) e^{ikr_j(1 - \hat{k} \cdot \hat{r}_j)} + \text{c.c.}, \end{aligned} \quad (1)$$

where c.c. is the complex conjugate of the first term.

Using the Tong-Huang-Wei (THW) inversion,¹⁰ $\Phi(\hat{k}, \mathbf{R})$ can be obtained by a Fourier-like transform of each $\chi(k, \hat{k})$ function:

$$\begin{aligned} \Phi(\hat{k}, \mathbf{R}) &= \int_{k_{\min}}^{k_{\max}} \chi(k, \hat{k}) e^{-ikR(1 - \hat{k} \cdot \hat{R})} dk, \\ &= \int_{k_{\min}}^{k_{\max}} A(\mathbf{k}, \hat{r}_j) e^{-ik[R(1 - \hat{k} \cdot \hat{R}) - r_j(1 - \hat{k} \cdot \hat{r}_j)]} dk. \end{aligned} \quad (2)$$

The second line is just the THW inversion of Eq. (1) without the c.c. term. \mathbf{R} is the real-space variable, and the final and initial points of a measured spectrum interval are k_{\max} and k_{\min} . For a finite interval a window function is used to control termination errors. For simplicity, this window function is not shown in the equation, and neither is the sum over the set of the j scatterers.

The atomic image function $U(\mathbf{R})$ can be obtained by transforming against the emission angle; this is a sum, since the data are collected for a uniform set of direction \hat{k} :

$$U(\mathbf{R}) = \left| \sum_{\hat{k} \in \text{Cone}(-\mathbf{R}, w)} \Phi(\hat{k}, \mathbf{R}) \right|^2. \quad (3)$$

As discussed elsewhere² the sum uses the small cone method. All the emission directions \hat{k} , which are uniformly distributed over the emission hemisphere, are grouped into bunches forming small cones of width w , whose central ray is “swept” over the hemisphere. The parameter w may range from one spectrum (delta cone) to all spectra on the full hemisphere (π). Usually a value around 30° yields an image with minimum artifacts. $U(\mathbf{R})$ has a maximum amplitude when $\mathbf{R} = \mathbf{r}_j$, as can be seen in Eqs. (2) and (3). $U(\mathbf{R})$ does not have a maximum amplitude from the c.c. term in Eq. (1).

Now let us take the derivative of function χ [Eq. (1)], with respect to the wave number k :

$$\begin{aligned} \frac{d\chi(k, \hat{k})}{dk} &= \frac{dA(\mathbf{k}, \hat{r}_j)}{dk} [e^{ikr_j(1-\hat{k}\cdot\hat{r}_j)}] \\ &+ A(\mathbf{k}, \hat{r}_j)(ir_j(1-\hat{k}\cdot\hat{r}_j))e^{ikr_j(1-\hat{k}\cdot\hat{r}_j)} + \text{c.c.} \end{aligned} \quad (4)$$

Here c.c. is the complex conjugates of the first and second terms. Now, replacing $\chi(k, \hat{k})$ with $d\chi(k, \hat{k})/dk$ without the c.c. term in the Tong-Huang-Wei transform [Eq. (2)], the derivative inversion field $\Phi^d(\hat{k}, \mathbf{R})$ becomes

$$\begin{aligned} \Phi^d(\hat{k}, \mathbf{R}) &= \int_{k_{\min}}^{k_{\max}} \left[\frac{dA(\mathbf{k}, \hat{r}_j)}{dk} \right] e^{-ik[R(1-\hat{k}\cdot\hat{R}) - r_j(1-\hat{k}\cdot\hat{r}_j)]} dk \\ &+ \int_{k_{\min}}^{k_{\max}} (ir_j(1-\hat{k}\cdot\hat{r}_j))A(\mathbf{k}, \hat{r}_j) \\ &\times e^{-ik[R(1-\hat{k}\cdot\hat{R}) - r_j(1-\hat{k}\cdot\hat{r}_j)]} dk. \end{aligned} \quad (5)$$

Similar to the behavior of $\Phi(\hat{k}, \mathbf{R})$, it is found that $\Phi^d(\hat{k}, \mathbf{R})$ has a maximum amplitude when the condition $\mathbf{R} = \mathbf{r}_j$ is satisfied, i.e., the phase factor is zero. The transform described in Eq. (5) is the KDS transform.

In the small-cone method,² the \hat{k} directions are selected in the neighborhood of $-\hat{R}$, i.e., $\hat{k} \approx -\hat{R}$. Further, the inversion Φ^d has the highest intensity at $\mathbf{R} = \mathbf{r}_j$. That is to say, these high-intensity positions are emphasized in the small-cone method, where the backscattering condition $\hat{k} \approx -\hat{r}_j$ is naturally satisfied. Thus, the second term in Eq. (5) is proportional to the amplitude of $2\mathbf{r}_j$, which is essentially $2\mathbf{R}$.

In the other parts of space away from the scattering atoms, Φ^d has a weak intensity as the condition $\mathbf{R} = \mathbf{r}_j$ is not satisfied. Then the second term is not proportion to R and instead depends on the value of $r_j(1-\hat{k}\cdot\hat{r}_j)$. The term goes to zero for forward scattering, which would suppress the forward focusing peak which is usually a complication of inversion procedures. In addition, the first term in Eq. (5) for Φ^d

is obviously not proportional to r_j . Further, this first term is typically near zero if the scattering function $A(\mathbf{k}, \hat{r}_j)$ is nearly independent of k . When the window is 180° for the full hemisphere approach, \hat{k} is not limited to directions around \hat{R} , i.e., the condition $\hat{k} \approx -\hat{R}$ is not generally satisfied. In this case the second term in Eq. (5) depends on the value of $r_j(1-\hat{k}\cdot\hat{r}_j)$, and a simple behavior is not found. Therefore, the KDS transform is only effective for surface emitters when used together with the small-cone method, and an increased sensitivity is obtained for more distant neighbors in the atomic image.

After using the small-cone summation of Eq. (3) for the derivative, the image function, $U^d(\mathbf{R})$, one sees that is re-

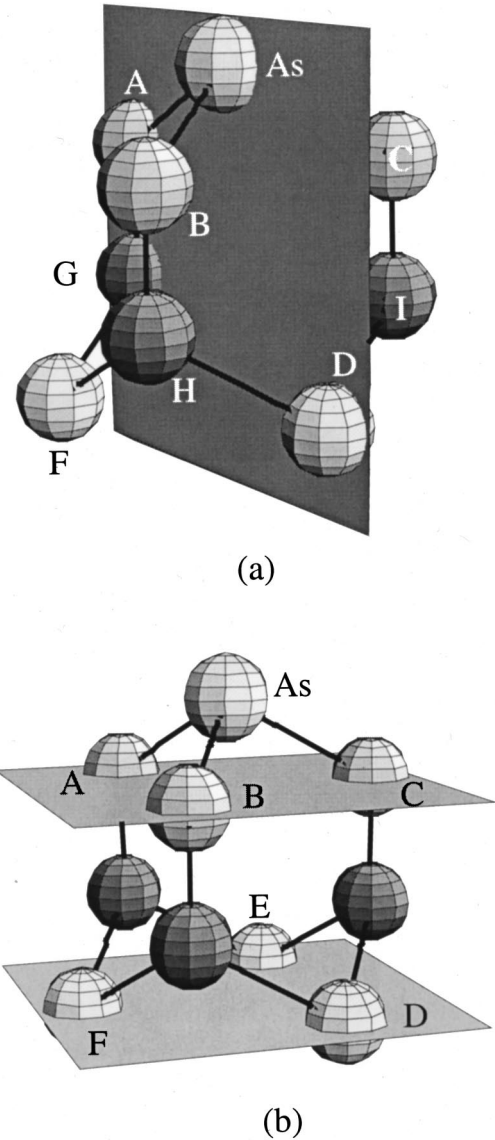


FIG. 1. 3D effective atomic structure for the As/Si(111) system. The arsenic atom replaces the top-layer Si atom, and bonds to Si atoms A, B, and C. Prior to this work, only A, B, C, and G were observed in images. (a) The vertical plane represents the X-Z planar cut shown in Figs. 2 and 3(a). (b) Two horizontal planes represent the X-Y planar cuts shown in Fig. 2 for Z at -0.9 and -4.1 Å.

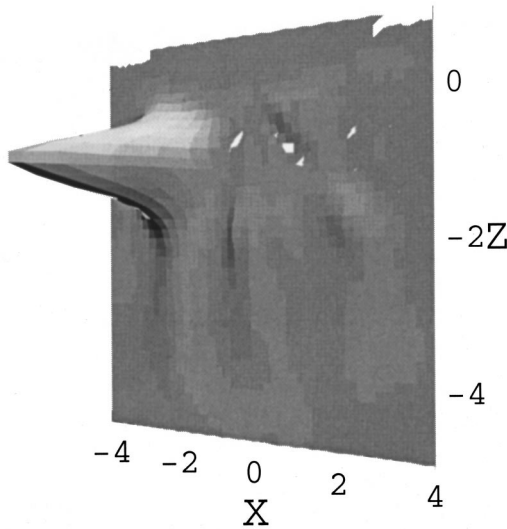


FIG. 2. The vertical X - Z planar cut of the As/Si(111) system obtained from the standard transform where the “third dimension” is the image intensity. The coordinate unit, Å. The emitter (As) is at the origin.

lated to $U(\mathbf{R})$ through $U^d(\mathbf{R}) \sim 4R^2 U(\mathbf{R})$. This relationship holds if, and only if, there is a scatterer at \mathbf{R} , that is, $\mathbf{R} = \mathbf{r}_j$. The image function $U(\mathbf{R})$ is obtained with the standard inversion, and $U^d(\mathbf{R})$ is obtained by the KDS transform. One can clearly see that the intensity is enhanced by R^2 comparing to the standard procedure. High-quality data are needed for a reliable derivative. The atomic image function $U^d(\mathbf{R})$

allows us to “see” more distant scatterers than the standard inversion function $U(\mathbf{R})$ for atoms at a surface.

The KDS inversions for several experimental PHD data sets as well as simulated PHD data sets have been examined. The KDS transform always obtains more distant scatterers. Here we present two experimental cases: a single-site emitter in the adsorbate case of As/Si(111), and a double-site emitter in the adsorbate case of C_2H_4 /Si(100). Note that, due to the phase shift in the electron scattering factor, the distance values may be distorted by $2/10$ – $3/10$ of an Å.²

Arsenic on a Si(111) surface has a well-known structure,^{4,13} in which the As atoms replace the Si atoms in the surface layer and bond to three Si atoms. Figure 1 presents this structure using the ball-stick model of atomic structure. In addition to traditional surface science investigations, two holographic imaging experiments have been reported on this system.^{4,13} Wu *et al.* obtained images which contained peaks of the first-layer Si atoms (A , B , and C).¹³ Luh *et al.* found peaks for the first-layer Si atoms and weak peaks for the second-layer Si atom (G) using a method for self-normalizing the constant-initial-energy spectrum data.⁴ Figure 2 shows the vertical planar cut obtained from the standard transform.¹³

In the present analysis, using the KDS transform we easily observe an image containing peaks due to the third-layer Si atoms (D , E , and F), as well as first- and second-layer Si atoms. Figure 3 presents the images obtained by the KDS transform. Peaks $A(B,C)$ are due to the first-layer Si atoms, peak G to the second-layer Si atom, and peaks $D(E,F)$ to the third-layer Si atoms. Their Z coordinate values are -0.9 ,

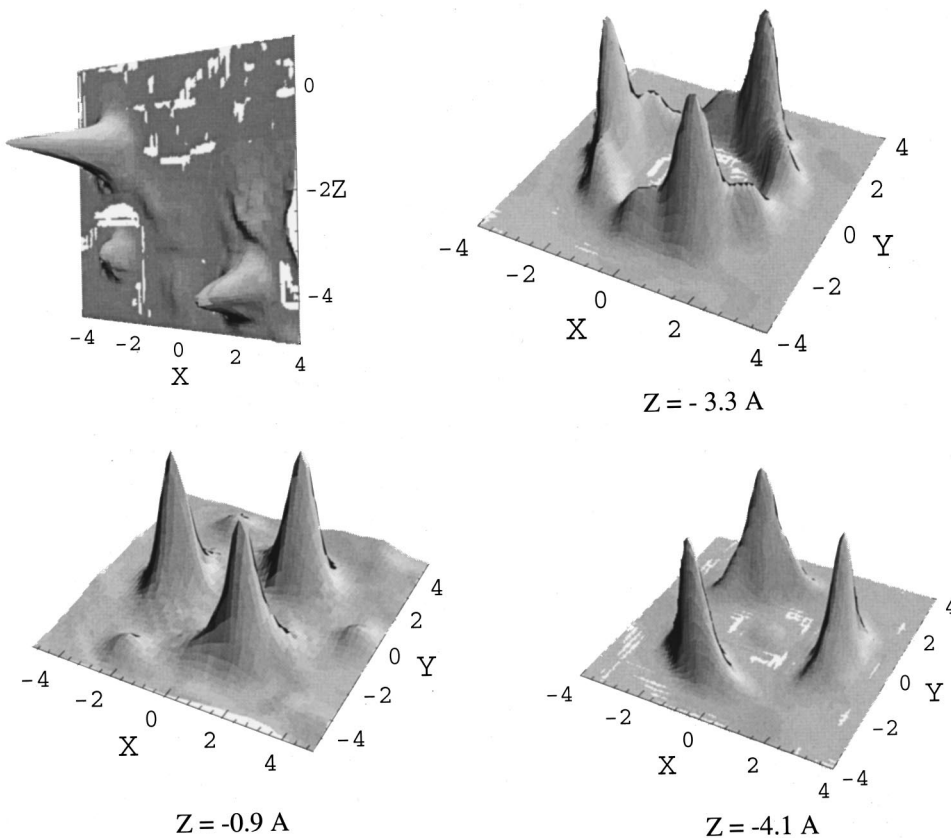


FIG. 3. Planar cuts of the atomic image of the As/Si(111) system obtained from the KDS transform, which show the intensity in the “third dimension.” The coordinate unit is Å. The arsenic emitter is at the origin, and the Si labels are from Fig. 1. The vertical (X - Z) planar cut appears in the upper left panel. The horizontal (X - Y) planar cut is at $Z = -0.95$ Å passing through Si atoms A and B . The horizontal (X - Y) planar cut is at $Z = -3.3$ Å passing through Si atoms G , H , and I . The horizontal (X - Y) planar cut is at $Z = -4.1$ Å, passing through Si atoms D , E , and F .

−3.3, and −4.1 Å, respectively. The values of their positions are in reasonable agreement with those known for a bulk Si crystal. The image peak for the third-layer Si atom (*D*) is very strong while the second-layer peak (*G*) is weak. In addition to the three strong peaks (*A*, *B*, and *C*) shown in Fig. 3 ($Z = -3.3$ Å), there are three weak peaks (*G*, *H*, and *I*) at $Z = -3.3$ Å in this image. Also, three weak peaks (not shown) are found due to the SNN Si atoms in the first Si layer. The peaks due to the third-layer Si atoms and the SNN Si atoms in the first layer are not observed in the images obtained by either the standard transform or the self-normalization transform.^{4,13} To our knowledge, this is the first time a PHI image for a single adsorption site reveals so many of the atoms neighboring the emitter.

In the case of the ethylene on Si(100) system, the two carbon atoms of the ethylene molecule each sit in inequivalent sites. In Ref. 5, reporting experiments, the molecule was found to sit atop a Si-Si dimer. When the standard transform was used, no other Si neighbors were observed. Figure 4 shows the ball-stick model for a PHI image model, where the two carbon atoms *P* and *Q* are placed at the origin. A proper atomic structure construction would have the carbon ball separated. The inversion places *all* emitters at the origin of the image. As discussed in Ref. 5, this makes it more difficult to make atomic assignments for the image peaks. The emitters (two carbon atoms in one ethylene molecule) are labeled *P* and *Q*, and a two-letter label is used for peaks in the image, e.g., *E/P* means Si atom *E* as “seen” by carbon emitter *P*. This work used a single-domain sample with double-high atomic steps. Recently the same site was reported by a “trial and error” comparison of photoelectron diffraction spectra with simulations¹⁴ for a two-domain sample.

Figure 4(b) shows an *X*-*Y* planar cut which passes through the second-layer Si atoms at $Z = -2.8$ Å. These atoms are the four strongest spots (*D/Q*, *E/P*, *F/P*, and *G/Q*) in the image. The *X* direction is parallel to the edge of the step, and hence parallel to the dimer bond. The *X* and *Y* coordinates of the spot *D/Q* are 1.2 and 1.9 Å, respectively. The spots form a rectangle. In the bulk crystal structure, however, they should form a square, ignoring any second-layer distortion due to the dimerization. The “double-exposed” rectangular image can be reduced to a square atomic structure by shifting peaks along the *X* direction until a square is formed. A ball-stick atomic structure could be constructed from Fig. 4(a) by imagining the ball *P/Q* to be two superimposed balls which could be separated to form the C_2H_4 “molecule” with concomitant shifts of the Si balls. The shift is 1.4 Å, and represents a carbon-carbon bond length in the ethylene molecule, which agrees with that of the free ethylene molecule (1.34 Å). From this length and the separation (0.6 Å) of the peaks due to the Si-Si dimer given in our paper,⁵ we obtain the Si-Si dimer bond length to be 2.0 Å, which is fairly close to the Si-Si dimer length (2.23 Å) of the clean Si(100) surface.¹⁵ This is direct evidence that ethylene adsorption does not break the Si-Si dimer bond, but only modifies the bond. The results essentially resolve one of the questions for ethylene adsorption.

In addition to the two cases mentioned above, the KDS

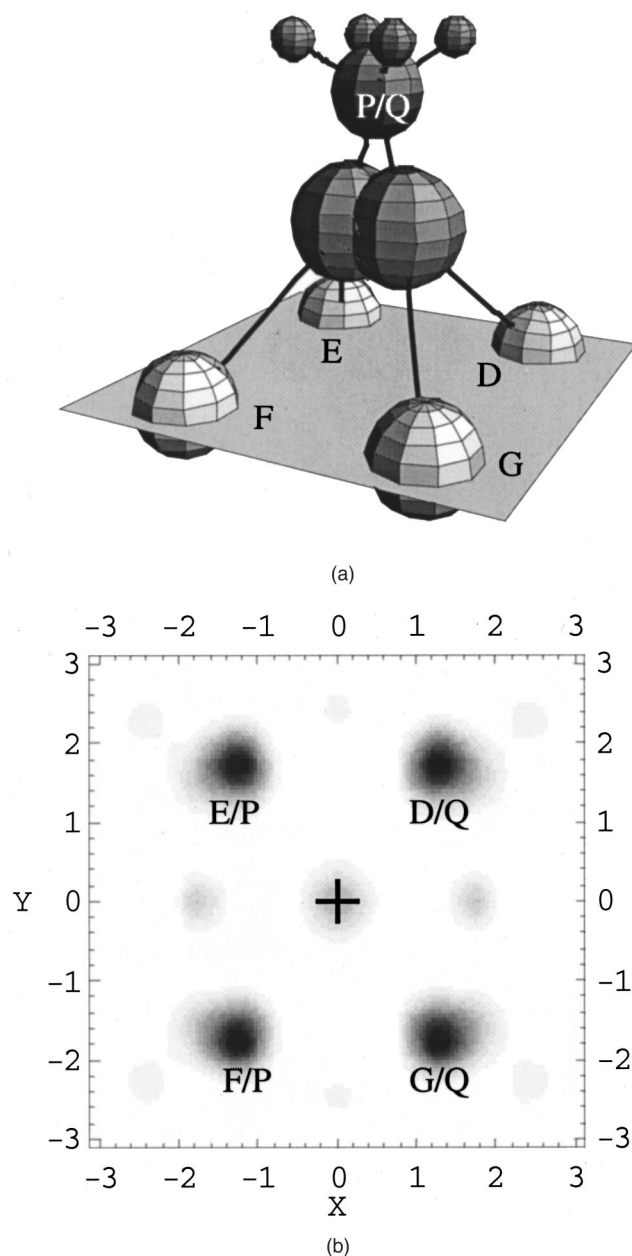


FIG. 4. (a) 3D effective image structure where the two inequivalent carbon emitters are both placed at the origin of the $C_2H_4/Si(100)-(2 \times 1)$ system. Small balls for hydrogen are added in geometrically likely positions based on the expected carbon hybridization. The (*P/Q*) ball represents the carbon atoms. The larger balls below represent the Si dimer atoms. Balls *D*, *E*, *F*, and *G* in the shaded horizontal plane are the Si atoms in second layer. (b) The *X*-*Y* plane cut at $Z = -2.8$ Å through the second-layer Si atoms obtained by the KDS transform. The four strong spots (*D/Q*, *E/P*, *F/P*, and *G/Q*) are due to the second-layer Si atoms. The coordinate unit is Å. (The other weak spots are due to the artifacts.) An atomic structure representation would be obtained by expanding the *X* direction (dimer bond direction) to obtain a square mesh for *E*, *D*, *F*, and *G*.

transform has been successfully used for other experimental and simulated PHD data. Thus, we conclude that the KDS transform is a new and very useful method to determine the atomic structure for atoms (adsorbate) at a surface.

In addition, if we take a second- or higher-order derivative of function χ with k , then the atomic image function would be enhanced by a higher power of R . It would seem that an image with even more distant scatterers would be seen. However, the derivative also “enhances” errors and noise. Hence the “cost” would be an increased precision in the data which would dramatically increase the measuring time.

The KDS transform used here is quite different from the self-normalization method proposed by Luh *et al.*⁴ although they sometimes called it the differential or derivative method. Luh *et al.* took the derivative of the PHD data with respect to the photon energy, and then integrated for a χ function. In pure mathematics, the derivative-integration cycle would not yield any change to the PHD data. As expected by Luh *et al.*,⁴ this process removes the discontinuities that may arise in the PHD data due to the limitations of the experimental condition such as shifts in the photon flux. In our method, however, we only use the derivative of the function χ instead of the differentiation-integration cycle. As expected by the theoretical approach, the images obtained by

the KDS transform can truly yield the more distant neighbors (scatterers).

In summary, the KDS transform is successfully used to construct atomic structures for the experimental systems As/Si(100) and C₂H₄/Si(100). This illustrates that in the holographic imaging method data are collected and inverted to directly obtain an image which needs to be inspected. No modeling is needed to obtain the adsorption site. In comparison with the standard transform, the images obtained by the KDS transform can yield more distant neighbors (scatterers). The KDS images unequivocally confirm the As adsorption site, and directly show that ethylene adsorption does not break the Si dimer bond. Several investigators suggest the dimer bond is broken. At the same time, no strong artifacts are observed in the images. Therefore, the KDS transform can be widely used for adsorbate systems.

The authors would like to thank the staff at SRC and ALS for their most generous help and support. This work was supported by the DOE and ONR DEPSCoR. The synchrotron facilities are supported by NSF and DoE, respectively.

*FAX: 406-994-4452. Electronic address: lapeyre@physics.montana.edu

¹H. Wu, G. J. Lapeyre, H. Huang, and S. Y. Tong, Phys. Rev. Lett. **71**, 251 (1993).

²Huasheng Wu and G. J. Lapeyre, Phys. Rev. B **51**, 14 549 (1995), and references therein.

³M. A. Mendez *et al.*, Phys. Rev. B **45**, 9402 (1992).

⁴D.-A. Luh *et al.*, Phys. Rev. Lett. **81**, 4160 (1998), and references therein.

⁵S. H. Xu *et al.*, Phys. Rev. Lett. **84**, 939 (2000).

⁶J. G. Tobin *et al.*, Surf. Sci. **334**, 263 (1995).

⁷P. M. Len *et al.*, Phys. Rev. B **59**, 5857 (1999).

⁸J. J. Barton, Phys. Rev. Lett. **67**, 3106 (1991).

⁹L. J. Terminello *et al.*, Phys. Rev. Lett. **70**, 599 (1993).

¹⁰S. Y. Tong, H. Huang, and C. M. Wei, Phys. Rev. B **46**, 2452 (1992), and references therein.

¹¹K.-M. Schindler *et al.*, Phys. Rev. Lett. **71**, 2054 (1993).

¹²The derivative method was presented at the 2000 March APS meeting and the Electron Spectroscopy and Structure Conference in Berkeley, CA (August of 2000). At the latter conference the C.S. Fadly group presented essentially the same derivative method with application for the control of the forward focusing peaks in data analysis for an emitter in the bulk.

¹³H. Wu *et al.* (unpublished); their work about As adsorption on Si(111) and Si(100) surfaces will be submitted; H. Wu, Ph.D. thesis, MSU-Bozeman, 1994.

¹⁴R. Terborg *et al.*, Phys. Rev. B **61**, 16 697 (2000).

¹⁵N. Roberts and R. J. Needs, Surf. Sci. **236**, 112 (1990).